Quantitative analysis of aluminium alloys by low-energy, high-repetition rate laser-induced breakdown spectroscopy

Gabriele Cristoforetti,*[a] Stefano Legnaioli,[a] Vincenzo Palleschi,[a] Azenio Salvetti,[a] Elisabetta Tognoni,[a] Pier Alberto Benedetti,[a] Franco Brioschi[b] and Fabio Ferrario[b]

Received 30th March 2006, Accepted 24th May 2006
First published as an Advance Article on the web 8th June 2006
DOI: 10.1039/b604628b

With the aim of reducing the dimensions of a laser-induced breakdown spectroscopy (LIBS) apparatus for building a portable instrument, a diode-pumped Nd:YAG mini-laser at high repetition rate was tested as an excitation source for the quantitative analysis of aluminium alloy samples. Moreover, LIBS spectra acquired by using an ICCD-echelle spectrometer detection system were compared with those obtained by a traditional spectrometer coupled to a non-intensified linear array detector. Calibration curves were built and limits of detections were calculated using both detection systems for magnesium, silicon, copper, titanium, manganese, nickel and iron. The results were compared with those obtained by recently proposed LIBS systems based on the use of microchip lasers.

Introduction

In recent years, the laser-induced breakdown spectroscopy (LIBS) technique has been established as a popular analytical tool for the determination of the elemental composition of materials[1] because of its intrinsic simplicity, its applicability to all phases of materials without sample preparation and the relative low-cost of instrumentation. Moreover, the quickness of the LIBS method together with the requirement of a mere optical contact of the probe (the laser beam) with the target, make it appropriate for *in situ* analysis, ranging from online monitoring of industrial processes,[2,3] environmental protection,[4,5] cultural heritage conservation[6,7] and even measurements in hostile environments.[8–11] In particular, LIBS performs best for low-Z elements than other hand held units such as X-ray fluorescence (XRF).[12] For these reasons, recently, a large effort has been made by the scientific community to reduce the dimensions of the LIBS apparatus toward the realization of portable instruments.

A step forward in this direction is the use of passively Q-switched microchips[13,14] as laser sources; in fact, since they do not require any switching electronics, these lasers are more compact and less complex than traditional systems, allowing the reduction of encumbrance of experimental apparatus to possible miniaturized setups. Though the pulse energy is usually in the range of tens of μJ, the high quality of the beam in microchip lasers allows one to produce an irradiance on the target similar to that obtained with other laser systems typically used in LIBS (in the range of 10^9–10^{11} W cm^{-2}). In the microchip lasers, the extremely short cavity length of several hundred micrometers produces pulse widths well below 1 ns and the passive Q-switch results in a repetition rate in the KHz range. The short laser duration results also in a plasma emission lifetime shorter than 1 ns, as found by Gornushkin *et al.*,[15] who used a 550 ps pulse of 7 μJ energy on several matrices and found a ~0.8 ns plasma luminous lifetime and a continuum level markedly lower than in traditional ns pulses in the mJ range. A few papers have been published on the applications of passively Q-switched microchips in laser-induced breakdown spectroscopy.[15–18] Freedman *et al.*[18] and Lopez-Moreno *et al.*[17] investigated the applicability of microchip lasers in quantitative LIBS analyses of aluminium alloys and low-alloy steel respectively. While in the first case the limits of detection (in the 0.05–0.14% range) were found to be poorer than required for a proper alloy classification, in the latter the limits of detection were lower than 100 ppm for most of the chemical elements studied and therefore competitive with traditional LIBS systems.

In this paper we probed the potentialities of the LIBS analysis using an electronically Q-switched Nd:YAG mini-laser emitting pulses of 9 ns FWHM at the fundamental wavelength of 1064 nm at a repetition rate in the kHz range. Though it is not strictly a microchip, the laser is still compact and thus competitive for portable LIBS instruments, since it is diode-pumped and air-cooled. Moreover, the combination of nanosecond pulse duration and kHz repetition rate makes the investigation of such a laser source for LIBS analysis interesting. In fact, Klimentov *et al.*[19] found that using a ns laser, for repetition rates higher than 4 kHz (and laser fluences of 100 J cm^{-2}) the ablation rates on a steel target are higher and similar to those obtained in vacuum. The authors attribute this effect to a reduced laser shielding of the subsequent pulses produced by the hot rarefied gas plume, thus resulting in a condition very similar to that obtained in double pulse LIBS configurations.[20,21]

In our experiment, the laser-ablation characteristics expected for this source are close to those found by Geertsen

[a] *Institute for Chemical–Physical Processes, Research Area of National Research Council, Via G. Moruzzi 1, 56124 Pisa, Italy. E-mail: gabriele@ipcf.cnr.it; Fax: +39 0503152230; Tel: +39 050315222*
[b] *Quanta System s.p.a., Via IV novembre 116, 21058 Solbiate Olona (VA), Italy*

et al.[22] and Cravetchi *et al.*,[23] who used traditional nanosecond laser sources with pulse energies in the μJ range. On the other hand, the high repetition rate and the laser fluence on the surface, are comparable to those of sub-nanosecond microchip lasers: this suggests to the experimentalist the possibility of testing non-intensified detectors as successfully adopted in microchip laser experiments.

In the present paper, an echelle spectrometer coupled to an intensified CCD and a Czerny–Turner spectrometer coupled to a non-intensified linear array detector were also tested and compared as detection systems in the LIBS portable prototype. The measurements were made on 10 certified aluminium alloys and calibration curves were built for several chemical elements ranging from the ppm to the percent concentration.

Experimental

Laser and focusing

The laser source is a diode pumped Nd:YAG prototype from Quanta System emitting at the fundamental wavelength (1064 nm). The diode-pumping and the air-cooling are effective in reducing the size of the laser source to dimensions comparable to the ones of commercial microchip lasers. The laser is triggered by a pulse generator (SRS, model DS345). The laser pulse energy can be varied by changing the diode–pump energy. The pulse energy and FWHM depend on the repetition rate as shown in Fig. 1, where the maximum diode–pump energy was used. For optimizing both the parameters, a frequency of 8 kHz was chosen, which allowed one to obtain a maximum laser power of ~9 kW per pulse, with a pulse energy of ~80 μJ and a FWHM of ~9 ns. The laser stability was monitored by sending a small fraction of the laser beam to a fast photodiode coupled to a digital oscilloscope, resulting in a RSD for the pulse energy of about 4%.

The beam was focused on the target surface by means of a microscope objective of 1.5 cm focal length, obtaining a laser spot on the target of diameter ~15 μm and an irradiance of about 5×10^9 W cm^{-2}.

The target was positioned on a rotating disk placed on a computer controlled *X*–*Z* micrometric translation stage. Similarly to that found in microchip ablation experiments,[16] the rotation of the target was necessary to sustain the plasma formation. In fact, focussing repeatedly the laser beam on the same spot leads to the disappearance of the plasma after less than 1 s of ablation (which corresponds to less than 8000 laser pulses).

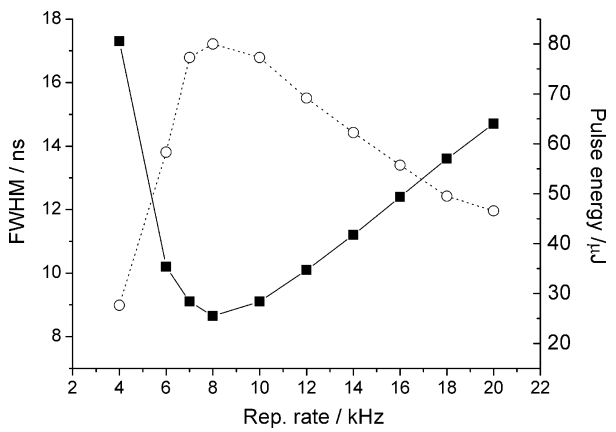

Fig. 1 Laser pulse width (squares, left axis) and energy (hollow circles, right axis) *versus* the laser repetition rate.

The craters drilled by laser ablation on the aluminium target were observed by video confocal microscopy. In Fig. 2a the image of a crater obtained by focusing the 8 kHz laser beam in the same point for 1 s is shown. In Fig. 2b the craters obtained by rotating the target at an angular velocity (~4 Hz) (for which the single holes are clearly separated) are shown.

It is evident that the crater obtained by focusing thousands of pulses on the same spot is much larger (~2–3 times in diameter) and much deeper than that obtained by a single pulse; moreover in the craters in Fig. 2b, the typical rim around the craters, generated by melt flushing in the drilling process, is visible by video confocal microscopy observation. The rim is, on the contrary, absent in Fig. 2a, suggesting that successive laser pulses vaporize the material previously solidified on the crater edge and enlarge the crater size.

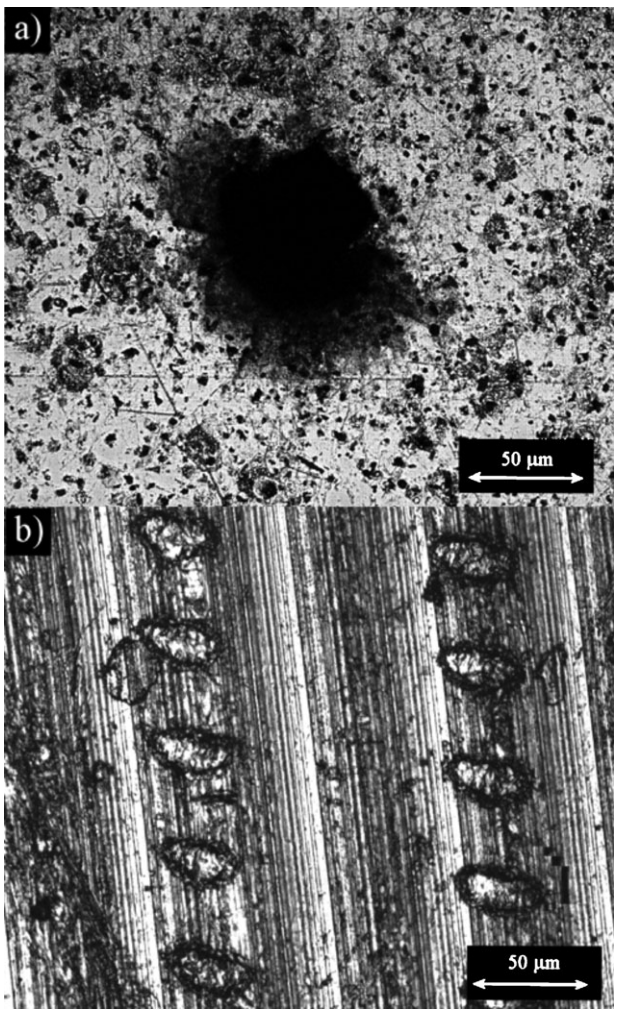

Fig. 2 Video confocal microscopy images of (a) a crater obtained by irradiating ~8000 laser shots on the same spot and (b) a series of single shot craters obtained by rotating the target during irradiation.

The disappearance of plasma after less than 1 s of consecutive ablation on the same spot is not related to thermic effects since the ablation does not occur again in the same crater after stopping and re-starting the laser after several seconds. On the other hand, it is not related to reflectivity changes of the surface since it would imply a disappearance of plasma after a single shot. Finally, it cannot be caused by the presence of aerosol in the air in front of the target, since the effect does not disappear by blowing a gas jet during the ablation process.

Thus, probably the cause of plasma disappearance is in the progressive de-focusing of the laser pulse at the lowering of the crater bottom during the consecutive ablations and in the optical masking of the beam by the sides of the crater. This problem is also shared by conventional LIBS system using microscope objectives but in this case it is made worst by the fact that the high repetition rate of the laser leads to the disappearance of the plasma in fractions of seconds.

The rotation velocity of the target was chosen with the purpose to obtain single shot craters well separated in space from each other; moreover a lateral movement was added to avoid the repeated ablation of the same circular path.

Acquisition and detector

The LIBS signal was collected through a quartz optical system of 10 cm focal length, placed at 45° with respect to the beam axis, and sent to the spectrometer through an optical quartz fibre (diameter = 600 μm, numerical aperture = 0.22).

In order to choose the optimal acquisition timing, the plasma lifetime was studied using a monochromator (Jobin-Yvon THR1000) coupled to a phototube (Hamamatsu R928). The phototube signal was observed with a digital oscilloscope. In Fig. 3 the temporal evolution of the continuum emission (~340 nm) of a neutral (Al I 396.1 nm) and of a ionic (Al II 358.6 nm) aluminium line after a laser pulse is reported. As in typical LIBS measurements, the lifetime of continuum emission (Δt ~13 ns) and of ionic lines (Δt ~ 24 ns) is much shorter than that of neutral lines (Δt ~ 80 ns). With respect to LIBS experiments where more energetic pulses are used, however, the plasma lifetime is 2–3 orders of magnitude shorter. Another interesting feature evident from Fig. 3 is the much smaller emission of continuum with respect to that obtained with traditional lasers in the mJ energy range (*i.e.* see ref. 23), according to what was found in microchip laser ablation experiments by Gornushkin *et al.*[15]

This last observation suggests the feasibility of using non-gated acquisition mode, with clear advantages in terms of cost and robustness of the apparatus.

It is interesting to note that the plasma emission lifetime, although much shorter than in classical LIBS, is nevertheless much longer than that usually obtained with microchip lasers. From the results published in the literature it is not clear how the time-integrated emission obtained with a ns laser compares with that produced with a ps laser at a constant fluence in the 10–100 J cm^{-2} range. In fact, although several papers reported that a much longer emission lifetime, a higher removal of material and higher plasma temperature are obtained by using ns lasers with respect to sub-nanosecond ones,[24–27] very few works compared the time integrated emission intensity in the two cases.[26,28]

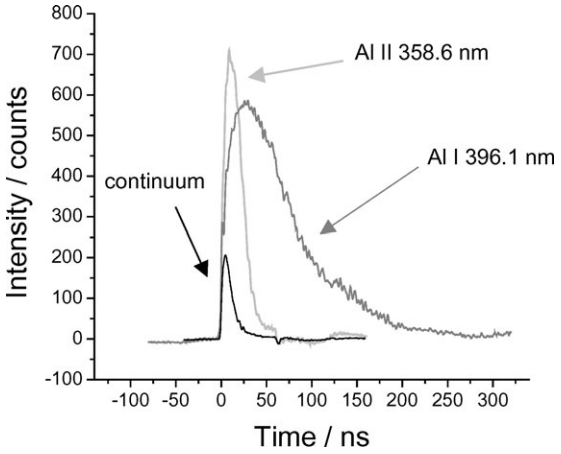

Fig. 3 Temporal profile of continuum emission (~340 nm) and neutral (Al I 396.1 nm) and ionic (Al II 358.6 nm) aluminium lines. The zero of the *x*-axis indicates the firing of the laser pulse.

As mentioned above, two different detection systems were used and compared for the quantitative analysis: an echelle spectrometer (Mechelle Instruments, $\lambda/\Delta\lambda$ = 7500) coupled to an intensified CCD camera (range 200–900 nm) and a portable spectrometer (AvaSpec 2048FT-SPU, $\Delta\lambda$ = 0.3 nm, range 170–439 nm) coupled to a non-intensified linear array.

In the first case, for each sample we averaged 4000 expositions of 10 ms for a total acquisition gate of 40 s, while in the latter we averaged 500 expositions of 40 ms for a total acquisition gate of 20 s. However, it is important to remark that the total time spent in the spectra acquisition in the case of the ICCD-echelle system is more than 10 times longer than the exposition time, due to the read out time of the two-dimensional CCD which is typically of the order of fractions of a second.

Moreover, it should be noticed that a longer measurement time leads also to a higher deterioration of the target due to a larger number of laser craters.

Results and discussion

In order to probe the potentiality of such experimental apparatus for quantitative LIBS analysis, we used 10 certified aluminium alloys containing also magnesium, nickel, iron, silicon, manganese, copper and titanium at different concentrations ranging from some ppm up to some percent.

In Fig. 4 an example of spectra obtained with both the spectrometers is shown. It is evident that the ICCD-echelle system allows one to resolve more clearly the adjacent line peaks since it has a higher spectral resolution (compare for example the Si I lines at 251.6 nm).

On the other hand, an advantage of using the portable spectrometer is its fastness and compactness. Moreover, although the signal to background ratio obtained with the two apparatus is similar, the lower noise level of the portable spectrometer provides a correspondingly higher signal to noise ratio for equal acquisition gates.

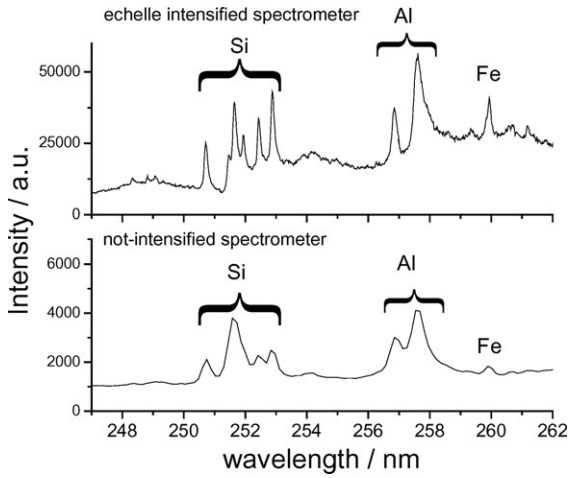

Fig. 4 A portion of LIBS spectra obtained with the two detection system.

The calibration curves were built for magnesium, nickel, iron, silicon, manganese, copper and titanium using the lines listed in Table 1. Because of the different efficiency curves of the two detectors, different lines were used for the determination of Fe concentration in the two cases while the Ni was observed only by using the echelle spectrometer.

For all the trace elements analysed, the peak intensity of the lines was normalized to the peak intensity of the Al I 256.8 nm line, thereby forming a ratio less sensitive to the shot-to-shot variations in the amount of ablated mass and in the plasma conditions. In the method of internal standard, it is preferable to normalize the line of the element studied with a line characterized by a similar upper energy level, resulting in a ratio less sensitive to the plasma temperature variations. Unfortunately, in the case of aluminium alloy, the range of available lines for the normalization is quite small. The Al I 256.8 line was chosen because it was the least intense among the highly visible Al lines, suggesting a reduced effect of self absorption. In fact, the 394.4/396.1 nm Al I doublet, although characterized by an upper energy level closer to that of Ni I, Cu I and Ti II lines, was rejected for its tendency to become self-absorbed.

In Fig. 5 and 6 the calibration curves of Cu, Mg and Mn obtained with the echelle and the portable spectrometer are reported, respectively. In all the cases, the points corresponding to self-absorbed lines, identified from an evident saturation of the intensity, were not plotted in the graph and not considered in the linear regression. The accuracy of the calibration can be estimated from the correlation coefficients R^2 of the linear regression, reported in Table 2. The accuracy of the calibration curves of Mn, Mg and Si are very high, probably because of the similarity of the upper level energies of their lines to that of the aluminium line, thereby compensating the emission variations due to the matrix effect. The same criterion can explain the poorer accuracy obtained for Cu and Ti, using the intensified and non-intensified spectrometer respectively, since the upper level energies of these lines are the most far from that of the aluminium line.

Table 2 Limits of detection and correlation coefficients calculated for all the trace elements in both the experimental setups

	Intensified spectrometer		Non-intensified spectrometer	
Species	R^2	LOD (ppm)	R^2	LOD (ppm)
Cu	0.859	122	0.970	17
Fe	0.945	405	0.950	137
Mn	0.990	180	0.990	67
Ni	0.958	490	—	—
Si	0.970	240	0.980	135
Ti	0.935	222	0.869	140
Mg	0.987	8	0.994	2

The limits of detection were calculated with the standard IUPAC method LOD = $3\sigma_B/s$ where σ_B is the noise level at the wavelength considered and s is the slope of the calibration curve at the lowest concentration of the analyte detected. Here, since a proper blank aluminium sample was unavailable, the noise level was calculated as the standard deviation of the background signal at a wavelength close to the measured line (and normalized to the same Al line used for building the calibration curves). The slope was calculated by fitting the data with a straight line, eventually after getting rid of the data in the saturation regime.

The LODs calculated for the two experimental setups are tabulated in Table 2. It is evident that the linear non-intensified detector provides better LODs (by a factor ranging from 2 to 7) compared to the ICCD-echelle system. Moreover, the LODs found with this apparatus are similar or just slightly poorer than those found in aluminium matrices with traditional LIBS setups (compare for example with refs. 29–31). On the contrary, they are much better (by a factor 10–100) than those obtained in aluminium alloys with microchip systems,[17] thus suggesting that the longer duration of the laser pulse in our apparatus could play a determining role in obtaining a stronger LIBS signal.

Table 1 Spectral parameters of the lines used in the calibration curves for the different elements

Species	Wavelength/nm	$A_{21}/10^8$ s^{-1}	E_1/cm^{-1}	g_1	E_2/cm^{-1}	g_2	Detector
Mg II	280.3	2.6	0	2	35 669	2	Both
Fe I	373.5	0.902	6928	11	33 695	11	Echelle sp.
Fe I	302.0	0.402	0	9	33 096	9	Portable sp.
Mn II	259.4	2.68	0	7	38 543	7	Both
Ni I	352.5	1.0	205	7	28 569	5	Echelle sp.
Cu I	324.7	1.37	0	2	30 784	4	Both
Ti II	334.9	1.33	393	10	30 241	12	Both
Si I	288.1	1.89	630	5	40 992	3	Both
Al I	256.8	0.23	0	2	38 929	4	Both

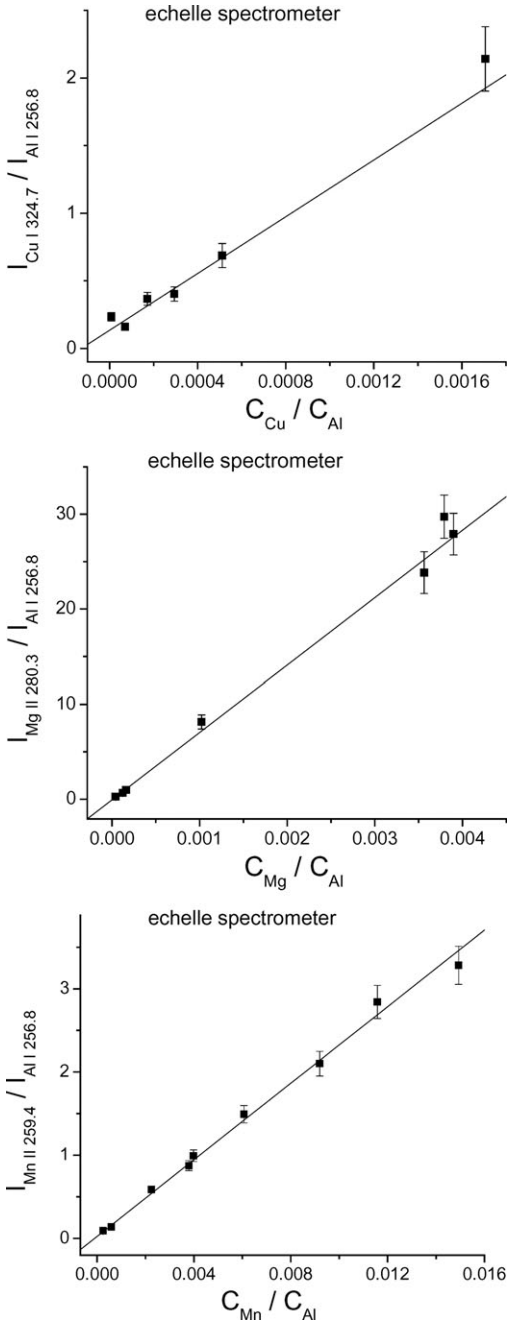

Fig. 5 Calibration curves of Cu, Mg and Mn obtained with the ICCD-echelle spectrometer system.

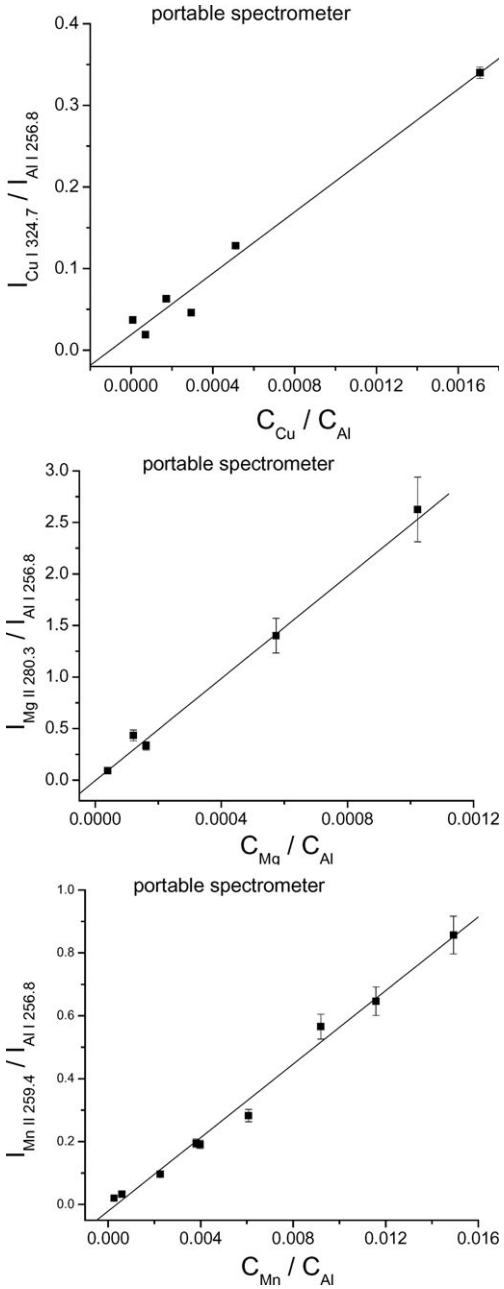

Fig. 6 Calibration curves of Cu, Mg and Mn obtained with the non-intensified linear array mini-spectrometer. In the Mg curve the points corresponding to the higher concentrations were not plotted since the intensities saturated the detector.

The results suggest that such a LIBS setup, built by using a diode-pumped mini-laser at high repetition rate and a compact low-cost non-intensified spectrometer, realizes an effective compromise between the system miniaturization characterizing the microchip-using LIBS apparatus and the better analytical performance of traditional LIBS systems using ns-lasers. It is also worth mentioning that higher resolving power non-intensified spectrometers can be utilized (evidently at the expense of the spectral band observed), which is necessary for analysing spectra with many emission lines such as those obtained by iron-based matrices.

Such a compact LIBS apparatus would be therefore of considerable smaller dimensions and weight with respect to the presently available mobile LIBS instruments, while maintaining similar analytical figures of merit.

Conclusions

In this work, a diode-pumped mini-laser at high repetition rate has been tested as laser source in a laser-induced breakdown spectroscopy setup. The attempt was motivated by the necessity of reducing the dimensions of the experimental apparatus

in view of building a portable LIBS prototype for *in situ* measurements. Moreover, since the high repetition of the laser source, in the range of kHz, involved non-gated acquisition of the signal , the performance of an ICCD-echelle detection system was compared with that of a portable non-intensified mini spectrometer, much smaller, faster and less expensive than the echelle.

Quantitative analysis was performed on ten certified aluminium samples, containing magnesium, manganese, iron, silicon, nickel, titanium and copper in traces; calibration curves were built and limits of detection were calculated for all the trace elements in both the experimental configurations. The limits of detection obtained by using the intensified detector, because of the higher level of the noise present in the spectra, are a factor 2 to 7 poorer than those obtained with the non-intensified detector. In this latter case the LODs were in the range of tens of ppm, comparable with typical values obtained with traditional LIBS setups.

The results therefore indicated that it is possible to build a truly portable LIBS setup, of considerable smaller dimensions and weight with respect to the presently available mobile LIBS instruments, while maintaining analytical figures of merit similar to those of traditional LIBS laboratory systems.

Acknowledgements

The present activity was performed in the framework of the MIAO (Microsensors for Analysis in Hostile Environment) project, funded by the Italian Ministry for Education and Research under the FIRB scheme.

References

1 E. Tognoni, V. Palleschi, M. Corsi and G. Cristoforetti, *Spectrochim. Acta, Part B*, 2002, **57**, 1115–1130.
2 R. Noll, H. Bette, A. Brysch, M. Kraushaar, I. Monch, L. Peter and V. Sturm, *Spectrochim. Acta, Part B*, 2001, **57**, 637–649.
3 H. Bette and R. Noll, *J. Phys. D: Appl. Phys.*, 2004, **37**, 1281–1288.
4 M. P. Mateo, G. Nicolas, V. Pinon, J. C. Alvarez, A. Ramil and A. Yanez, *Anal. Chim. Acta*, 2004, **524**, 27–32.
5 G. A. Lithgow, A. L. Robinson and S. G. Buckley, *Atmos. Environ.*, 2004, **38**, 3319–3328.
6 S. Klein, T. Stratoudaki, V. Zafiropulos, J. Hildenhagen and K. Dickmann, *Appl. Phys. A: Mater. Sci. Process.*, 1999, **69**, 441–444.
7 F. Colao, R. Fantoni, V. Lazic, L. Caneve, A. Giardini and V. Spizzichino, *J. Anal. At. Spectrom.*, 2004, **19**, 502–504.
8 S. Lawson, J. Wright, J. Young and A. Whitehouse, *Nucl. Eng. Int.*, 2000, **45**, 22–23.
9 U. Panne, R. E. Neuhauser, C. Haisch, H. Fink and R. Niessner, *Appl. Spectrosc.*, 2003, **56**, 375–380.
10 P. L. Garcia, J. M. Vadillo and J. J. Laserna, *Appl. Spectrosc.*, 2004, **58**, 1347–1352.
11 B. Salle, J. L. Lacour, E. Vors, P. Fichet, S. Maurice, D. A. Cremers and R. C. Wiens, *Spectrochim. Acta, Part B*, 2004, **59**, 1413–1422.
12 X. Hou and B. T. Jones, *Microchem. J.*, 2000, **66**, 115–145.
13 S. Zhou, K. K. Lee, Y. C. Chen and S. Li, *Opt. Lett.*, 1993, **18**, 511–512.
14 J. J. Zayhowski and C. Dill III, *Opt. Lett.*, 1994, **19**, 1427–1429.
15 I. B. Gornushkin, K. Amponsah-Manager, B. W. Smith, N. Omenetto and J. D. Winefordner, *Appl. Spectrosc.*, 2004, **58**, 762–768.
16 K. Amponsah-Manager, N. Omenetto, B. W. Smith, I. B. Gornushkin and J. D. Winefordner, *J. Anal. At. Spectrom.*, 2005, **20**, 544–551.
17 C. Lopez-Moreno, K. Amponsah-Manager, B. W. Smith, I. B. Gornushkin, N. Omenetto, S. Palanco, J. J. Laserna and J. D. Winefordner, *J. Anal. At. Spectrom.*, 2005, **20**, 552–556.
18 A. Freedman, F. J. Iannarilli, Jr and J. C. Wormhoudt, *Spectrochim. Acta, Part B*, 2005, **60**, 1076–1082.
19 S. M. Klimentov, P. A. Pivovarov, V. I. Konov, D. Breitling and F. Dausinger, *Quantum Electron.*, 2004, **34**, 537–540.
20 M. Corsi, G. Cristoforetti, M. Giuffrida, M. Hidalgo, S. Legnaioli, V. Palleschi, A. Salvetti, E. Tognoni and C. Vallebona, *Spectrochim. Acta, Part B*, 2004, **59**, 723–735.
21 G. Cristoforetti, S. Legnaioli, V. Palleschi, A. Salvetti and E. Tognoni, *Spectrochim. Acta, Part B*, 2004, **59**, 1907–1917.
22 C. Geertsen, J. L. Lacour, P. Mauchien and L. Pierrard, *Spectrochim. Acta, Part B*, 1996, **51**, 1403–1416.
23 I. V. Cravetchi, M. Taschuk, G. W. Rieger, Y. Y. Tsui and R. Fedosejevs, *Appl. Opt.*, 2003, **42**, 6138–6146.
24 M. Corsi, G. Cristoforetti, M. Hidalgo, D. Iriarte, S. Legnaioli, V. Palleschi, A. Salvetti and E. Tognoni, *Appl. Spectrosc.*, 2003, **57**, 715–721.
25 A. Semerok, C. Chaleard, V. Detalle, J.-L. Lacour, P. Mauchien, P. Meynadier, C. Nouvellon, B. Sallé, P. Palianov, M. Perdrix and G. Petite, *Appl. Surf. Sci.*, 1999, **138–139**, 311–314.
26 P. Stavropoulos, C. Palagas, G. N. Angelopoulos, D. N. Papamantellos and S. Couris, *Spectrochim. Acta, Part B*, 2004, **59**, 1885–1892.
27 J. Jandeleit, A. Horn, R. Weichenhain, E. W. Kreutz and R. Poprawe, *Appl. Surf. Sci.*, 1998, **127–129**, 885–891.
28 G. W. Rieger, M. Taschuk, Y. Y. Tsui and R. Fedosejevs, *Spectrochim. Acta, Part B*, 2003, **58**, 497–510.
29 M. A. Ismail, G. Cristoforetti, S. Legnaioli, L. Pardini, V. Palleschi, A. Salvetti, E. Tognoni and M. A. Harith, *Anal. Bioanal. Chem.*, 2006, **385**(2), 316–325.
30 M. Sabsabi and P. Cielo, *Appl. Spectrosc.*, 1995, **49**, 499–507.
31 A. K. Rai, H. Zhang, F. Y. Yueh, J. P. Singh and A. Weisburg, *Spectrochim. Acta, Part B*, 2001, **56**, 2371–238.

